Z. Physik B 26, 1–10 (1977)

Zeitschrift
für Physik B

On the Electronic Structure of Graphite

J. Kieser
Physikalisches Institut, Universität Karlsruhe, Fed. Rep. Germany

Received October 7, 1976

Comprehending investigations of the electronic structure of polycrystalline as well as monocrystalline graphite have been performed by means of X-ray emission, self absorption and X-ray induced photoemission techniques. On the basis of these combined investigations a model for the determination of the relative cross sections for the photoemission process has been established and applied to graphite, where it yields $\sigma_s/\sigma_p = 32$. The anisotropy and polarization of the C K-radiation of monocrystalline graphite is discussed in terms of the binding properties of the graphite lattice. The predictions are verified by measurements of the C K-emission employing a crystal monochromator which acts simultaneously as a nearly perfect analyzer for the polarization of the monochromatized radiation. By means of the self absorption technique the unoccupied part of the conduction band has been investigated.

I. Introduction

The presented paper deals with a comprehending investigation of the electronic properties of graphite, employing the techniques of X-ray emission and absorption spectroscopy and X-ray induced photoemission spectroscopy. This investigation is especially interesting due to the extreme anisotropy of the graphite lattice, which determines the electronic structure of the valence as well as the conduction band. Additionally the lattice anisotropy should yield an anisotropy and polarization of the X-ray spectra.

Graphite exhibits a layered structure, where the monolayers consist of hexagonal arrays of atoms. The bonds between the layers are weak and mainly due to van der Waals interactions. The bonds in the layers are considerably stronger. They result mainly from σ-bonds, which evolve from the so called sp^2 hybridisation of three occupied orbitals per atom, namely the $2s$, $2p_x$ and $2p_y$ orbital. The three binding directions of these covalent σ-bonds are coplanar and exhibit bonding angles of 120°, thus causing the hexagonal structure in the monolayers. Additional binding between all pairs of next neighbours is contributed by the π-bonds, which evolve from occupied p_z orbitals.

The electronic properties of graphite, especially the electronic density of states $N(E)$ in the valence and conduction band are essentially determined by its bonding properties.

Calculations of the band structure of graphite have been frequently performed [1–4]. The most reliable theoretical investigation seems to be the calculation performed by Painter and Ellis [1], since their band structure shows good agreement with the results of investigations of the optical properties of graphite by Greenaway et al. [5], though no experimentally determined fitting parameters have been used for the calculation. From this can be concluded that the calculation [1] should be essentially correct.

On the basis of this band structure Brümmer et al. [6] have deduced the $N(E)$-structure for the valence band, which is composed of two partly overlapping σ- and π-subbands.

Since the σ-subband evolves from atomic wavefunctions with s- and p-symmetry, it contains s- and p-like states. In this sense the π-band contains only p-like states.

For the investigation of $N(E)$ in a greater range around the Fermi level the traditional Soft X-ray Emission Spectroscopy (SXS) and X-ray Absorption Spectroscopy (XAS) can be employed, observing the dipole selection rule $\Delta l = \pm 1$. Carbon has only one inner niveau, namely the $1s$-niveau. Therefore the

SXS- and XAS-spectra as are shown in Section III probe the partial density of p-like states.

Recently the X-ray induced Photoemission Spectroscopy (XPS) has been developed as tool for the investigation of the electronic density of states. The results of an XPS-investigation are presented and discussed in terms of the s-like partial density of states. Therefore an approximation of the $N(E)$-structure by a linear combination of the measured SXS- and XPS-spectra has been tried. On this basis a model calculation has been performed, which yields the relative cross sections for the photoemission process in valence and conduction bands.

Due to the different charge distributions of the σ- and π-bonds in the graphite lattice the emission spectrum from monocrystalline graphite should show different anisotropy as well as polarization properties of the σ- and π-subbands resp. The investigation of these properties was possible by the successful growth of an organic single crystal with a suitable lattice constant. Due to this lattice constant the C K-spectrum could be investigated employing Bragg angles of approx. 45°, which are close to the Brewster angle for X-rays. The monochromator acts in this case simultaneously as an analyser for the polarization of the investigated radiation. Corresponding investigations are discussed in Section IV.

II. Experimental

1. Apparatus

The spectrometer consists of stainless steel. During the measurements a vacuum of $p < 4 \times 10^{-9}$ Torr was generated by ion getter pumps. The used spectrometer geometry has been described by Eggs and Ulmer [7].

As monochromators spherically bent organic single crystals according to Eggs and Ulmer [7] have been used. The measurements on polycrystalline carbon were performed with a Dioctadecyladipate-OAO-crystal, while for the anisotropy and polarization measurements an Octadecyl-Hydrogen-Maleate – (OHM)-crystal has been used. The investigated C K-spectrum covers an energy range of approx. 284–262 eV. This corresponds to a range of Bragg angles of approx. 27°–31° for the OAO- and 43°–48° for the OHM-monochromator, corresponding to a double lattice spacing of $2d_{OAO} = 90.55$ Å [8] and $2d_{OHM} = 63.39$ Å [9].

A resolution of 0.5 eV was obtained considering all resolution determining geometric factors.

The photoemission measurements have been performed in an ESCA-3 apparatus (Fa. Vacuum Generators). As exciting radiation $Al_{K\alpha 1,2}$-radiation has been used. For further details compare Kieser and Trogus [10].

2. Samples

For the X-ray spectroscopic measurements on polycrystalline graphite small rods of pyrolytic graphite with the dimensions $30 \times 1 \times 0.1\ mm^3$ have been used. The rods were mounted under angles of approx. 15° relative to the direction to the monochromator. This yielded an effective width of the entrance slit of approx. 0.2 mm.

For the monocrystalline measurements different samples have been used:

Samples with the dimensions $7 \times 1 \times 1\ mm^3$ have been prepared from natural graphite. The cleaved surface exhibited dislocations of approx. ±6°. Therefore additional samples have been prepared by smearing natural graphite onto the surface of tungsten ribbons.

Within the measuring accuracy both preparation techniques yielded the same results.

3. Relevant Properties of the Monochromator Crystals

The systematic application of organic single crystals as monochromators for the ultrasoft X-ray region requires the investigation of the relevant properties of these monochromators.

A principal limitation of the energy resolution of a Bragg reflecting single crystal follows from the finite number of reflecting planes, due to the absorption in the crystal. An estimation based on a treatment given by Compton and Allison [11] yielded that approx. 600 planes take part in the reflection in the considered energy range. Therefore no significant loss of energy resolution due to the absorption in the monochromator is expected.

Since the employed monochromator crystals contain carbon, their reflectivity in the considered energy range and especially near the C K-absorption has been subject to separate investigation.

A sharp decrease near 287 eV has been found in the otherwise nearly constant reflectivity. This can be interpreted in terms of an onset of C K-absorption. The energy of this C K-absorption is approx. 3 eV greater than the corresponding edge in graphite, which is 284.3 eV according to Johansson et al. [12] and Kieser and Kleber [13].

This result is in agreement with theoretical as well as experimental investigations of the C 1s binding energy in some organic molecules by Davis and Shirley [14] and Gelius et al. [15].

The C K-absorption in the monochromator therefore does not influence the measurement of the C K-spectrum.

4. Analysing Properties of the Monochromator

The polarizability of X-rays has first been shown by Barkla [16] and be confirmed by Compton and Hagenow [17]. Accordingly the polarization of X-rays can be investigated with methods, commonly used in optics, if a refraction index $n=1$ is employed. This result seems to justify the transfer of the relevant optical laws to the energy range of X-rays as is performed in the following.

The usefulness of the monochromator as analyser for polarized X-rays is determined by the employed Bragg angle.

According to Brewster's law

$$\tan \alpha_p = n \tag{1}$$

(α_p = angle of incidence)

a wave incident with α_p, which is polarized in the plane of incidence, is not reflected.

In the energy range of interest $n=1$ is valid in very good approximation (compare, e.g., Compton and Allison [11]), from which follows $\alpha_p = 45°$. For Bragg reflection under $\phi_B = 45°$ this component in the incoming radiation should therefore be absorbed in the crystal.

In this work an energy range $260\,\text{eV} \leqq E \leqq 295\,\text{eV}$ is investigated, corresponding to Bragg angles $48.8 \geqq \phi_B \geqq 41.4°$.

The analysing properties of the monochromator in this range are determined by the Fresnel equations.

If one observes $\alpha = \beta$, due to $n=1$, where β is the angle of the refracted beam, their application yields*

$$P = \frac{1-(\cos 2\alpha)^2}{1+(\cos 2\alpha)^2} \tag{2}$$

where P is the degree of polarization of the reflected radiation.

Together with $\phi_B = 90° - \alpha$, (2) yields $P \geqq 0.966$ for the employed range of Bragg angles, the monochromator is therefore a nearly perfect analyser in the investigated energy range.

III. Polycrystalline Graphite

1. Emission Spectrum

The emission spectrum of polycrystalline graphite is well known. According measurements with an OAO-crystal monochromator have therefore been performed in order to test its usefulness. Further the energy resolution of the used crystal monochromator, as compared to gratings usually employed in this energy region, can be expected to be better. This should be helpful in elucidating the problem of the degree of overlapping of the subbands.

* The intensity of the braggreflected radiation is not affected in this case, in contrast to optical reflection

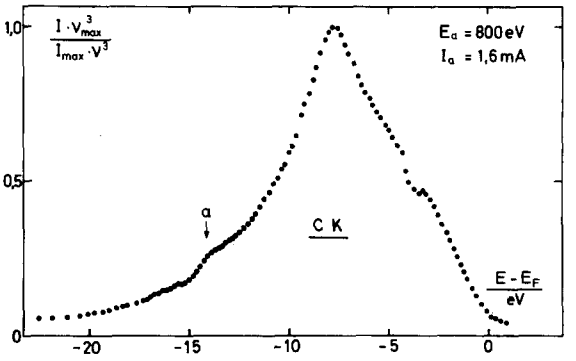

Fig. 1. C K-spectrum from pyrolytic graphite, recorded with an OAO-crystal

Figure 1 shows a C K-emission spectrum of pyrolytic graphite. It is comparable to more recent measurements by Sagawa [18], Holliday [19] and Brümmer et al. [6], who employed gratings as monochromator. The high energetic part of the spectrum including the so called π-maximum at -3.1 eV results from the π-subband, while the low energetic part is mainly determined by the σ-subband.

The position of the Fermi level follows from the calibration of the spectrometer together with the value of the binding energy of the 1s-niveau $E^B_{C\,1s} = 284.3$ eV [12, 13]. Accordingly the σ-maximum lies at 276.6 eV in accordance with a value of 277 ± 0.3 eV given by Bearden [20].

Sagawa [18] finds as a result of an unfolding of his spectrum that the σ- and π-subbands in the valence band are well separated. Though the resolution of the spectrometer in the presented investigation was considerably better (FWHM $\simeq 0.5$ eV) as compared to the FWHM = 2.7 eV, given by Sagawa, the presented spectrum shows rather strong overlap of the subbands. This is in accordance with a rejection of Sagawas analysis by Ergun and Weisweiler [21], based on a discussion of his unfolding procedure.

The relative energetic position of the π-maximum at -3.1 eV is comparable with the measurements [6, 18, 19], but its relative height differs significantly. Typical differences of approx. 10% due to the used sample have been found. On the basis of the concept of different anisotropy of the radiation from the σ- and π-components this can be explained in terms of different degrees of crystalline order in the investigated samples. This concept is strongly supported by the results obtained from spectra of monocrystalline graphite, as is discussed in Section IV.

According to this concept the height of the π-peaks in samples of polycrystalline graphite as compared to amorph samples should be different, as has been observed by Holliday [19].

The structure in the spectrum of Figure 1, labelled with 'a' is possibly due to the electronic density of states. On the other hand its generation by the well known characteristic energy loss of 6.8 eV (compare, e.g., Marton and Leder [22], Zeppenfeld [23]) cannot be excluded.*

2. Self Absorption Spectrum (SAS)

The technique of SAS yields results comparable to the results of classical X-ray absorption – (XAS)-measurements. But in contrast to XAS, self absorption measurements can be performed on thick samples. As a further advantage the self absorption spectrum can be obtained together with the corresponding emission spectrum simultaneously. The relative energy positions of both spectra are therefore correct, without any uncertainty as may be introduced by fitting procedures.

For the investigation of the electronic p-like structure of graphite in the poly- as well as monocrystalline modification this technique therefore seems to be exceptionally suitable.

The SAS-technique, as has been proposed by Liefeld [25] and dicussed by Umeno and Wiech [26] uses the self absorption of quanta, which are generated in the probe by means of primary or secondary excitation. The degree of self absorption is determined by the mean depth of generation of radiation.

For self absorption holds:

$$I(E)=I_0(E)\,e^{-\mu_r(E)\cdot\bar{x}} \tag{1}$$

where $I_0(E)$ is the intensity which is produced in the mean depth $\bar{x}$. $I(E)$ is the emitted intensity.

For two values of the primary excitation energy E_a and E_b follows:

$$I_a(E)=I_{0a}(E)\,e^{-\mu_r(E)\cdot\bar{x}_a} \tag{2}$$

$$I_b(E)=I_{0b}(e)\,e^{-\mu_r(E)\cdot\bar{x}_b} \tag{3}$$

(2) and (3) yield

$$\mu_r(E)\sim\ln\frac{I_a(E)}{I_b(E)}+\text{const.}$$

This result is valid under the assumption that the energy independent background can be neglected. On the other hand due to the presence of a constant background only a smearing of $\mu_r(E)$ is effected. Therefore the self absorption spectrum of graphite can be regarded within a simple model as a picture of the p-like density of states above the Fermi level, due to the dipole selection rule.

Figure 2 shows the high energetic part of the SXS-spectrum of Figure 1 together with the simultaneously measured self absorption spectrum. In the interesting energy region above the Fermi level only the continuum bremsstrahlung can be employed for the measurements. Due to its low intensity the investigation of self absorption spectra is very laborious if a conventional grating is employed and has not yet been performed for graphite. It should therefore be emphasized that one of the main advantages of the crystal monochromators as have been used in this work is the considerably higher intensity obtained in the investigated energy region as compared to gratings.

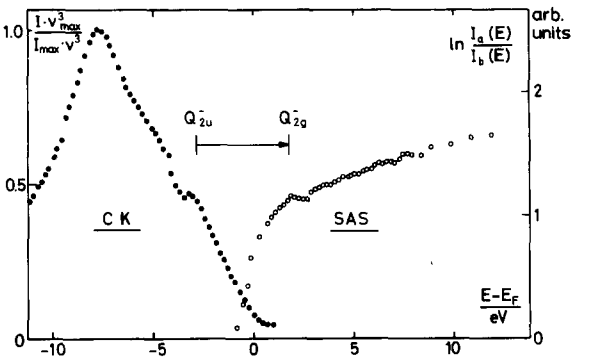

Fig. 2. Part of C K-spectrum and simultaneously measured self absorption spectrum. Excitation energies: $E_a=800$ eV, $E_b=2400$ eV. The position of an interband transition according to the bandstructure [1] is indicated

Near the Fermi level (E_F) the band structure of graphite is determined by the π-subbands [1–4], which exhibit a rather symmetric shape in respect to E_F. The self absorption curve should therefore be correlated with the electronic density of states generated by the unoccupied π-subband. The maximum in the self absorption spectrum at +2.0 eV is in good agreement with the $N(E)$-maximum to be expected at the point Q_{2g}^- in the band structure [1]. A further confirmation for this maximum is given by Kieser and Kleber [13], who measured the excitation curve of polycrystalline graphite.

In Figure 2 the relative positions of the points Q_{2g}^- and $Q_{2\mu}^-$ according to the calculation [1] are shown. The arrow indicates direct interband transitions of $\hbar\omega=4.6$ eV as have been observed by Greenaway et al. [5] and correlated with transitions $Q_{2u}^-\rightarrow Q_{2g}^-$.

The general agreement* with the energetic distance of both maxima further confirms that the maximum in the self absorption curve corresponds to a maximum in the electronic density of states of the unoccupied π-subband.

The intersection point of the spectra in Figure 2 does not represent the position of the Fermi level. This is

* A second characteristic energy loss of 27 eV has already been observed in the C K-spectrum by Aita et al. [24]

* For this transition holds $\Delta k=0$, the energetic positions of the two niveaus therefore need not be identical with the positions of the maxima in $N(E)$

possibly due to the arbitrary normalization of both π-maxima to the same height.

3. Photoemission Spectrum

The lower part of Figure 3 shows an XPS-spectrum measured by Kieser and Trogus [10]. The position of the Fermi level has been determined on the basis of a calibration with a gold standard with an estimated error of ± 0.4 eV. The upper part of Figure 3 shows for comparison the electronic density of states [1, 6]. Both curves exhibit good agreement as regards the bandwidths, in contrast to former measurements [27–29] and a more recent measurement [30]. On the other hand only the lower parts of both curves show some agreement. Since in this energy range the density of states should mainly be determined by the *s*-like density of states, the comparison of the curves suggests that the XPS-spectrum of graphite represents mainly the distribution of the *s*-like states. From this follows that the cross sections σ_s and σ_p for the photoemission process from the respective valence band states should be strongly different, where $\sigma_s \gg \sigma_p$.*

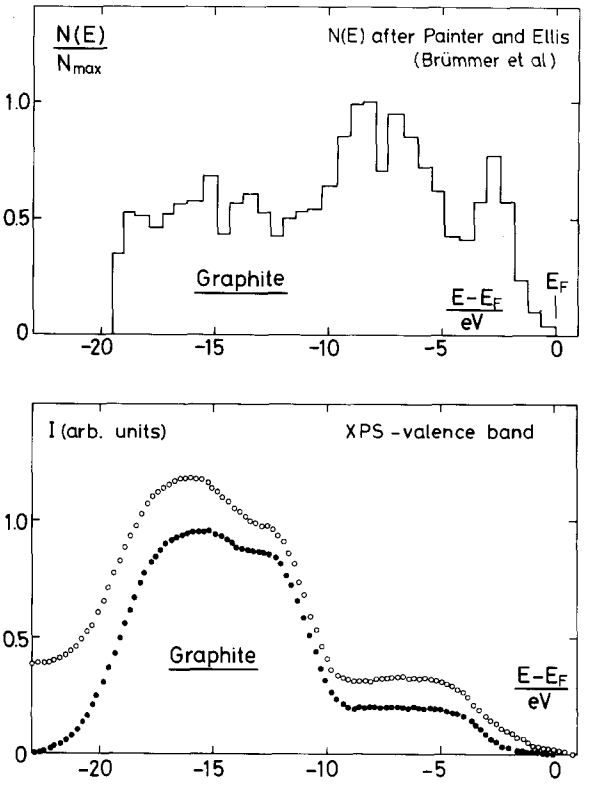

Fig. 3. Upper part: $N(E)$ after [1, 6], lower part: (oooo): measured XPS-valence band spectrum; (●●●●): XPS-valence band spectrum corrected for background as well as Al $K_{\alpha 3,4}$-satellites

4. The Relative Photoemission Cross Sections

The quantitative knowledge of the cross sections for the photoemission process is of basic importance for the comparison of XPS valence band measurements with calculated densities of states.

In the following a model is developed which yields on an experimental basis the quantitative determination of σ_s/σ_p. The model is restricted to valence bands which evolve from atomic wavefunctions with two different symmetries.

The problem of the relative cross sections for XPS-spectra from carbon has been investigated theoretically as well as experimentally for molecules by Hamrin et al. [31], Gelius [32], Price et al. [33], Cavell et al. [34] and Barfield et al. [35].

Hamrin et al. [31] found $\sigma_s/\sigma_p \simeq 13$** in an XPS-investigation on methane. In a recent work on the relative cross sections in the valence band of graphite Berg et al. [30] discussed values from 15 to 35 for σ_s/σ_p. A basic problem with regard to the determination of relative XPS-cross sections in the valence band of solids is connected with the hybridisation of band states with different symmetries. Due to this hybridisation it seems to be highly problematic to separate the valence band into regions with different symmetry, as has been performed by Cavell et al. [34] on the XPS-valence band spectra of diamond, silicon and germanium, in order to estimate the ratios σ_s/σ_p.

A theoretical estimation of the relative XPS-cross sections in solids is given by McFeely et al. [29] on the basis of a theory developed by Gelius [32] for molecules. Accordingly no great differences of the relative cross sections of free atoms as compared to solids should be expected.

This expectation, together with the experimental result [31] is a further confirmation that the XPS-spectrum of graphite is mainly determined by *s*-like states.

On the other hand due to the dipole selection rules the C *K*-emission spectrum represents the distribution of the *p*-like states in the valence band of graphite. Therefore an appropriate linear combination of the XPS- and SXS-spectra should represent the density of states as has been proposed by Kieser [37].

Such a comparison is shown in Figure 4. The good agreement can be improved if the density of states

* Here by σ_p the mean cross section for all *p*-like states in the valence band is denoted. Due to the different spatial distributions of the σ- and π-bonds different cross sections $\sigma_{p\sigma}$ and $\sigma_{p\pi}$ from the σ- and π-bonds respectively may be expected, as is discussed by Berg et al. [30]. But according to [30] this difference is not great in the case of a big value of σ_s/σ_p as is found in this work

** This value results from an XPS-spectrum obtained with unmonochromatized Al K_α-radiation. Consideration of the Al $K_{\alpha 3,4}$-satellites should yield a considerable enhancement of this ratio [36]

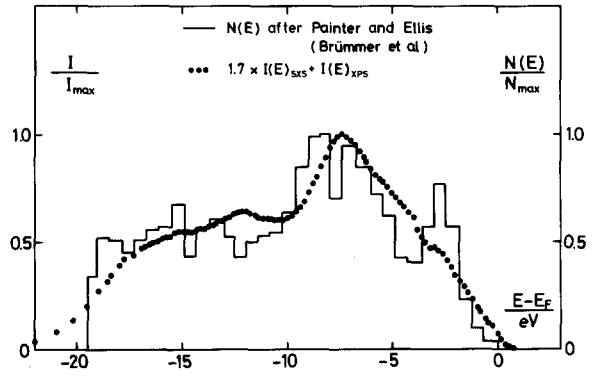

Fig. 4. Comparison of $N(E)$ after [1, 6] with a linear combination of an SXS- and XPS-spectrum. The respective $I(E)$-values were taken from the spectra after subtraction of the background and normalization of both spectra to the same area

structure between -5 eV and -10 eV is shifted approx. 1 eV towards the Fermi level, as has already partly been proposed by Kortela and Manne [38].

On the basis of the successful description of the density of states structure by the discussed linear combination a model calculation for the determination of the relative XPS-cross sections in valence bands of solids is performed.

Starting point is the model equation for the valence band of graphite:

$$N(E)=\alpha\cdot I(E)_{\mathrm{SXS}}+\beta\cdot I(E)_{\mathrm{XPS}}. \tag{1}$$

α and β are independent constants with the dimension $[1/I(E)\times$ number of occupied states/atom $\cdot$ eV$]$.

The $I(E)$ values result from the measured and normalized spectra with the normalization conditions

$$\int_{\mathrm{V.B.}} I(E)_{\mathrm{SXS}}\,dE=A \tag{2a}$$

$$\int_{\mathrm{V.B.}} I(E)_{\mathrm{XPS}}\,dE=A \tag{2b}$$

with $[A]=[I(E)]\cdot[E]$.

Integration of (1) over the valence band yields

$$\int_{\mathrm{V.B.}} N(E)\,dE=\alpha\int_{\mathrm{V.B.}} I(E)_{\mathrm{SXS}}\,dE+\beta\int_{\mathrm{V.B.}} I(E)_{\mathrm{XPS}}\,dE$$

$$N_s+N_p=\alpha\cdot A+\beta\cdot A.$$

N_s and N_p represent the number of s- and p-like electrons/atom respectively.

Considering the dipole selection rule it follows

$$I(E)_{\mathrm{SXS}}=O\cdot N_s(E)+\frac{A}{N_p}\cdot N_p(E). \tag{3a}$$

By the corresponding statement for $I(E)_{\mathrm{XPS}}$ the cross sections σ_s and σ_p are defined:

$$I(E)_{\mathrm{XPS}}=\mathrm{const}\cdot[\sigma_s\cdot N_s(E)+\sigma_p\cdot N_p(E)].$$

The constant can be evaluated on the basis of (2b).

It follows:

$$I(E)_{\mathrm{XPS}}=A\left[\frac{\sigma_s}{\sigma_s\cdot N_s+\sigma_p\cdot N_p}\cdot N_s(E)\right.$$

$$\left.+\frac{\sigma_p}{\sigma_s\cdot N_s+\sigma_p\cdot N_p}\cdot N_p(E)\right] \tag{3b}$$

(3a), (3b) and (1) yield

$$N(E)=\beta\cdot A\frac{\sigma_s}{\sigma_s\cdot N_s+\sigma_p\cdot N_p}N_s(E)$$

$$+\left[\frac{\alpha\cdot A}{N_p}+\beta\cdot A\frac{\sigma_p}{\sigma_s\cdot N_s+\sigma_p\cdot N_p}\right]N_p(E).$$

Since $N(E)=N_s(E)+N_p(E)$:

$$\beta\cdot A\frac{\sigma_s}{\sigma_s N_s+\sigma_p N_p}=1$$

$$\frac{\alpha\cdot A}{N_p}+\beta\cdot A\frac{\sigma_p}{\sigma_s\cdot N_s+\sigma_p\cdot N_p}=1.$$

From this follows

$$\frac{\sigma_s}{\sigma_p}=\frac{N_p\left(1+\frac{\alpha}{\beta}\right)}{N_p-\frac{\alpha}{\beta}\cdot N_s}. \tag{4}$$

For the best fit shown in Figure 4 $\alpha/\beta=1.7$ has been used. According to the sp^2-hybridisation in graphite one expects $N_p/N_s=3:1$. From a comparison of the partial p-like density of states of the graphite valence band by Kortela and Manne [38] with the total density of states [1, 6] more exact values of $N_p=2.6$ p-like and $N_s=1.4$ s-like states/atom can be deduced. With these values (4) yields $\sigma_s/\sigma_p=32$.

This result is in reasonable agreement with corresponding investigations on molecules [31] and is directly comparable to $\sigma_s/\sigma_p=34$ calculated by Barfield et al. [35] for free carbon atoms.

Completely independent from the discussed model calculation a lower limit for σ_s/σ_p can be deduced.

According to the SXS-spectrum the maximum of the p-like density of states is observed at -7.7 eV. The normalized intensity observed at this energy in the XPS-spectrum of Figure 3 is therefore an upper limit for the maximum of the p-like density of states in the XPS-spectrum. This consideration leads to a lower limit $\sigma_s/\sigma_p\geqq 11$.

No structure is observed in the XPS-spectrum at -7.7 eV. From this can be concluded that at the considered energy the maximum of the p-like density of states contributes only a small fraction to the observed intensity. From this follows that the value of σ_s/σ_p should be considerably greater than 11, in agreement with the performed model calculation.

The high value obtained for σ_s/σ_p is a confirmation for the expectation [29] of the basic agreement between the corresponding ratios in free atoms and solids.
Further the strongly different shape of the measured XPS-spectrum as compared to the XPS-spectrum calculated by Kortela and Manne [39] can essentially be explained in terms of a too low assumed value of σ_s/σ_p.

IV. Monocrystalline Graphite

1. Introduction

a) Bonding and Lattice Structure

In Graphite the so called σ-bonds between the atoms of a monolayer are mainly formed from sp^2-hybridized orbitals. The centers of gravity of the charge distribution of these bonds lie in the layer plane. An additional π-bond between the atoms of a monolayer is effected by the occupied p_z-orbitals. This bond is characterized by two centers of gravity of the charge distribution of an atom above and below the layer plane. The possible π-bonds of an atom to the 3 next neighbours are energetically equivalent.
According to Pauling [40] a resonance state involving one third double binding between all pairs of next neighbours is verified. From this can be concluded that the centers of gravity of the π-bond charge distribution are positioned exactly above and below the atoms.

b) Polarization and Anisotropy of the C *K*-Emission

According to the bonding properties of graphite the transition of an electron from the π-bond into the spherically symmetric 1*s*-state generates a dipole moment perpendicular to the layer plane. From this results the π-radiation which should be polarized parallel to the c-axis. Accordingly all directions of maximum intensity lie in the layer plane, while perpendicular to the layer plane no π-radiation should be emitted.
Transitions of electrons from the σ-bonds into 1*s*-states generate dipole moments in the layer plane. The corresponding σ-radiation is therefore polarized parallel to the layer planes and exhibits nonvanishing intensity in all directions.
First indications of an anisotropy of the C *K*-radiation have been found by Borovskii et al. [41], who employed a lead stearate as monochromator. Further measurements by Brümmer et al. [6], Müller et al. [42] and Beyreuther and Wiech [43], performed with better resolution confirmed this anisotropy.
Recently Beyreuther et al. [44] and Berg et al. [30] have determined the shapes and bandwidths of the π- and σ-subbands on the basis of the measurements of Beyreuther and Wiech [43].
Due to the successful growth of OHM-single crystals the direct measurement of the polarization of the C *K*-radiation was possible. In orienting measurements of the C *K*-spectra from different carbon samples McFarlane [45] found a considerable stronger dependence of the spectra from the relative sample orientation than [6, 41–43] from which a polarization of the C *K*-radiation can be concluded.
In the presented investigation on monocrystalline graphite the direct determination of the shapes and widths of the π- and σ-subbands is performed on the basis of the discussed polarization and anisotropy properties of graphite. Further the degree of polarization of the π-radiation as well as the polarization properties of the monochromator crystal are investigated.

2. Emission Spectra

a) π-Subband

The C $K\pi$-spectrum has been obtained with a mounting of the sample according to Figure 5a. In this position maximum intensity of the π-component propagates towards the monochromator. Additionally the electric field vector $\mathbf{E}_\pi$ is approximately perpendicular in respect to the Rowland circle plane, which is the plane of incidence. On the other hand the σ-radiation is suppressed, since $\mathbf{E}_\sigma$ lies in the plane of incidence.
The upper part of Figure 6 shows this C $K\pi$-spectrum. The position of the Fermi level has been determined as in the case of the polycrystalline measurements. The high energetic part of the spectrum shows excellent agreement with the corresponding part of the polycrystalline measurements of Figure 1.

b) σ-Subband

For the measurement of the C $K\sigma$-spectrum sample arrangements according to Figures 5b and c can be used.
In the arrangement according to Figure 5b no π-radiation propagates to the monochromator, due to its anisotropy. On the other hand $\mathbf{E}_\sigma$ is perpendicular to the plane of incidence. The σ-radiation is therefore reflected with maximum intensity. A spectrum measured with this arrangement is also shown in the upper part of Figure 6. The low energetic part of this spectrum is nearly identical with the polycrystalline spectrum of Figure 1.
In Figure 5c a further arrangement for the suppression of the π-radiation is demonstrated. Here $\mathbf{E}_\pi$ lies in the plane of incidence, while the emission of π-radiation towards the monochromator is nearly maximal. The suppression of the π-radiation is therefore dependent on the degree of its polarization and the corresponding analyzing properties of the monochromator.

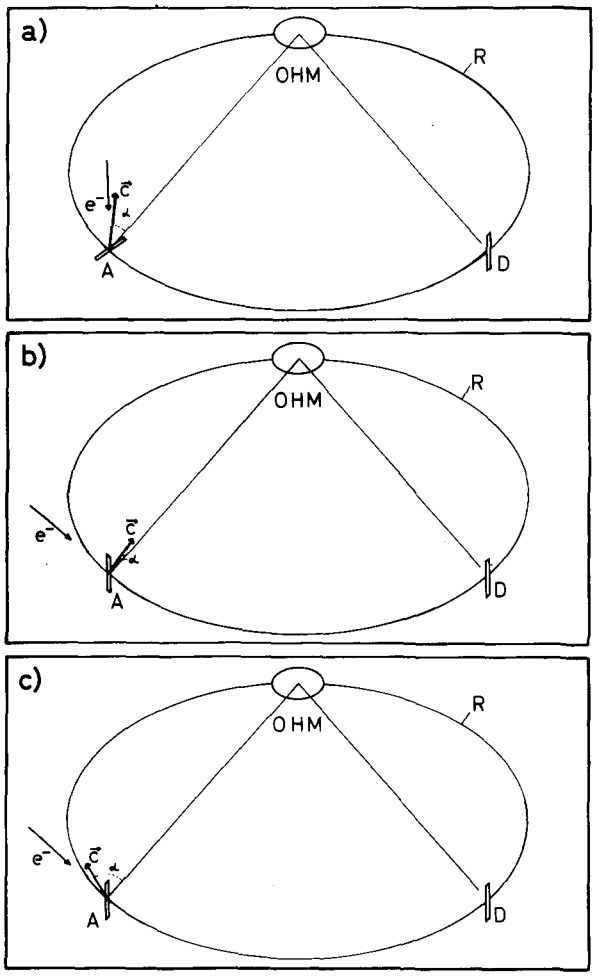

Fig. 5. Geometric arrangements of the c-axis (perpendicular to the layer planes) of the probe relative to the Rowland circle *R*. The direction of the exciting electron beam is indicated. a) $\alpha = 87°$; b) $\alpha = 3°$; c) $\alpha = 87°$

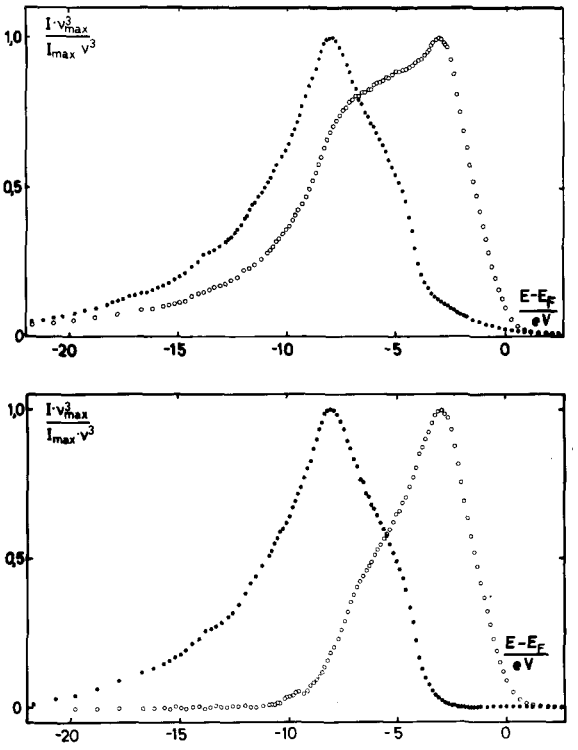

Fig. 6. Upper part: Measured C *K*-spectra of monocrystalline graphite obtained with different arrangements of the sample. (○○○○): π-spectrum obtained with an arrangement according to Figure 5a. (●●●●): σ-spectrum obtained with arrangements according to Figures 5b, c. Lower part: (○○○○): Corrected π-spectrum. (●●●●): Corrected σ-spectrum. All spectra are normalized to the same height. The Fermi level corresponds to the zero of energy

The spectrum obtained with this arrangement is within the experimental error identical with the spectrum obtained with the arrangement of Figure 5b. From this can be concluded that the π-radiation is completely polarized parallel to the *c*-axis. Further the entirely polarizing properties of the monochromator are confirmed, as has been expected on the basis of the Fresnel equations.

c) Discussion

The presented π- and σ-spectra show completely different shapes. From this can be concluded that the expectations concerning the anisotropy and polarization properties of the C *K*-radiation, based on the bonding properties in graphite, are confirmed. Especially the complete linear polarization of the π-radiation could be demonstrated.*

* The experimental confirmation of the linear polarization of the π-radiation shows the fundamental possibility to construct monochromatic, polarized X-ray sources for photoemission measurements without the use of a synchrotron.

The measured π- and σ-spectra shown in Figure 6 contain a small amount of the supressed component. This is mainly due to the used samples of natural graphite which were no perfect single crystals. Additionally even at the used UHV carbon containing contaminations were deposited on the sample which caused a progressive smearing of the investigated crystal structure. Therefore a simple correction procedure has been applied to the spectra.

According to Painter and Ellis [1] the overlap of the σ- and π-subbands is restricted to the high energetic part of the C *K*-spectrum. Therefore the low energetic tail of the π-spectrum should be generated by σ-electrons. Similarly the intensity present in the high energetic part of the σ-spectrum should be due to π-radiation. In order to correct for these intensities a fit of the σ-spectrum to the π-spectrum has been performed in the energy range $-23\,\text{eV} \leqq E \leqq -14\,\text{eV}$. The difference curve is shown in the lower part of Figure 6. It should be noted that its horizontal-part is not restricted to the fitting range.

The shape and bandwidth of the corrected π-spectrum can therefore be regarded to be essentially correct. It represents the electronic density of states of the oc-

cupied π-band if the X-ray transition probability is regarded to be energy independent.

Likewise the corrected σ-spectrum, as is also shown in the lower part of Figure 6, has been obtained. As fitting range $-2.7 \leqq E \leqq -1.5$ eV was employed in this case. It represents the p-like density of states of the σ-subband, possibly modified by the X-ray transition probability as well as Auger broadening.

The C K-spectrum can be discussed in terms of a superposition of the π- and σ-spectra. Therefore in Figure 7 the C K-spectrum of a polycrystalline graphite probe, obtained with the OHM-monochromator is compared to a linear combination of the corrected π- and σ-spectra. The excellent agreement of both curves strongly indicates that the shapes of the spectra as shown in the lower part of Figure 6 are essentially correct.

A comparison of the corrected spectra with the respective curves deduced from the measurements [43] by Berg et al. [30] and Beyreuther et al. [44] yields satisfactory agreement, especially as concerns the bandwidth of the π-subband. The obtained bandwidth of approx. 9.5 eV is 2 eV broader than the corresponding calculated value. Consequently the found overlap of 5.5 eV between π- and σ-subband is much greater than in the calculation (2.5 eV), in accordance with the discussion of the polycrystalline measurements (Section III).

As concerns the total valence bandwidth there exists some uncertainty. Berg et al. [30], who give a table of calculated values consider the bandwidth of 19.4 eV as given by Painter and Ellis [1] to be too low, since their XPS-spectrum is considerably broader.

This is in contrast to corresponding XPS-work by Kieser and Trogus [10], who investigated the influence of adsorbed oxygen on the graphite valence band spectrum. They obtained a bandwidth of approx. 20 eV from oxygen free graphite, while the presence of oxygen resulted in a distortion as well as broadening of the measured XPS-spectrum.

The C K-spectrum of Figure 1 likewise shows a bandwidth of about 20 eV, without any correction for the tailing due to Auger processes, in agreement with the C K-spectra of Beyreuther and Wiech [43]. As a consequence the comparison of the best fit of a linear combination of XPS- and SXS-spectrum to the calculated density of states [1, 6] as is shown in Figure 4 yields good agreement, especially with regard to the bandwidths.

3. *Self Absorption Spectrum*

Figure 8 shows a self absorption spectrum of monocrystalline graphite. A sample mounting according to Figure 5a has been employed.

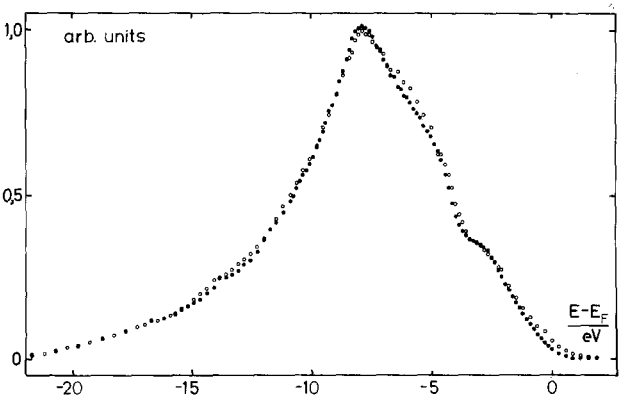

Fig. 7. Comparison of a C K-spectrum of pyrolytic graphite (oooo) obtained with an OHM-monochromator with a linear combination $\alpha \cdot I_\pi + \beta \cdot I_\sigma$ of the corrected π- and σ-spectra (●●●●); α and β have been chosen in such a way as to obtain the best fit of both curves

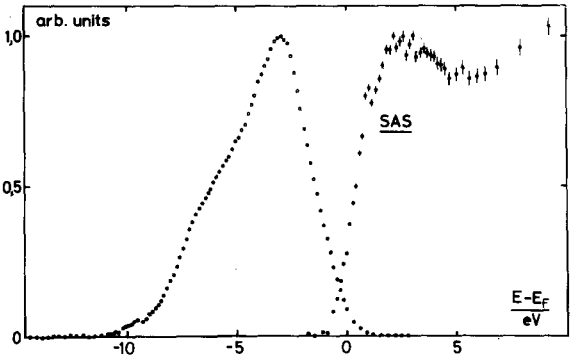

Fig. 8. Comparison of the corrected π-spectrum with the simultaneously measured self absorption spectrum of monocrystalline graphite. Both curves are normalized to the same height

In contrast to the according measurements on polycrystalline graphite the maximum of the unoccupied π-subband is considerably more pronounced, which can be explained in terms of a preferred absorption of X-rays polarized parallel to the c-axis. From this can be concluded that the connection of bounding properties and polarization of X-rays as has been discussed for the valence band of graphite is valid for the unoccupied part also.

I want to express my gratitude to Prof. Ulmer, who supported this work substantially by many discussions as well as by making available the monochromator crystals.
The performance of the measurements on monocrystalline graphite by cand. phys. R. Krätschmer is gratefully acknowledged.

References

1. Painter, G.S., Ellis, D.E.: Phys. Rev. B **1**, 4747 (1970)
2. Zupan, J.: Phys. Rev. B **6**, 2477 (1972)
3. Tsukada, M., Nakao, K., Uemura, Y., Nagai, S.: J. Phys. Soc. Japan **32**, 54 (1972)

4. Nagayoshi, H., Tsukada, M., Nakao, K., Uemura, Y.: J. Phys. Soc. Japan **35**, 396 (1973)
5. Greenaway, D.L., Harbeke, D., Bassani, F., Tosatti, E.: Phys. Rev. **178**, 1340 (1969)
6. Brümmer, O., Dräger, G., Fomichev, W.A., Schulakow, A.S. in: X-Ray Spectra and Electronic Structure of Matter, ed. A.Faessler and G. Wiech, München 1973, Vol. I, pp. 78–90
7. Eggs, J., Ulmer, K.: Z. angew. Physik **20**, 118 (1965)
8. Fischer, D.W.: Acta Cryst. **17**, 619 (1964)
9. Föll, H.: To be published
10. Kieser, J., Trogus, H.: Phys. Letters **48** A, 401 (1974)
11. Compton, A.H., Allison, S.K. in: X-Rays in Theory and Experiment (ed. A.H. Compton), pp. 391–394. Princeton-Toronto-New York-London: D. van Nostrand 1960
12. Johansson, G., Hedman, J., Berndtsson, A., Klasson, M., Nilsson, R.: J. Electron Spectroscopy **2**, 295 (1973)
13. Kieser, J., Kleber, R.: Appl. Phys. **9**, 315 (1976)
14. Davis, D.W., Shirley, D.A.: J. Electron Spectroscopy **3**, 137 (1974)
15. Gelius, U., Hedén, P.F., Hedman, J., Lindberg, B.J., Manne, R., Nordberg, R., Nordling, C., Siegbahn, K.: Physica Scripta **2**, 70 (1970)
16. Barkla, C.G.: Proc. Roy. Soc. **77**, 247 (1906)
17. Compton, H., Hagenow, C.F.: J. Opt. Soc. Am. and Rev. Sci. Instr. **8**, 487 (1924)
18. Sagawa, T.: J. Phys. Soc. Japan **21**, 49 (1966)
19. Holliday, J.E.: J. appl. physics **38**, 4720 (1967)
20. Bearden, J.A.: Rev. Modern Physics **39**, 78 (1967)
21. Ergun, S., Weisweiler, W.: Carbon **8**, 101 (1970)
22. Marton, L., Leder, L.B.: Phys. Rev. **94**, 203 (1954)
23. Zeppenfeld, K.: Z. Physik **211**, 391 (1968)
24. Aita, O., Nagakura, I., Sagawa, T.: J. Phys. Soc. Japan **30**, 516 (1971)
25. Liefeld, R.J. in: Soft X-Ray Band Spectra (ed. D.J. Fabian), pp. 133–149. London-New York: Academic Press 1968
26. Umeno, M., Wiech, G.: Phys. Stat. Sol. b **59**, 145 (1973)
27. Hamrin, K., Johannson, G., Gelius, U., Nordling, C., Siegbahn, K.: Physica Scripta **1**, 277 (1970)
28. Thomas, J.M., Evans, E.L., Barber, M., Swift, P.: Trans. Faraday Soc. **67**, 1875 (1971)
29. McFeely, F.R., Kowalczyk, S.P., Ley, L., Cavell, R.G., Pollak, R.A., Shirley, D.A.: Phys. Rev. B **9**, 5268 (1974)
30. Berg, U., Dräger, G., Brümmer, O.: Phys. Stat. Sol. b **74**, 341 (1976)
31. Hamrin, K., Johansson, G., Gelius, U., Fahlman, A., Nordling, C., Siegbahn, K.: Chemical Physics Letters **1**, 613 (1968)
32. Gelius, U. in: Electron Spectroscopy (ed. D.A. Shirley), pp. 311–334. Amsterdam-London: North Holland 1972
33. Price, W.C., Potts, A.W., Streets, D.G. in: Electron Spectroscopy (ed. D.A. Shirley), pp. 187–198. Amsterdam-London: North Holland 1972
34. Cavell, R.G., Kowalczyk, S.P., Ley, L., Pollak, R.A., Mills, B., Shirley, D.A., Perry, W.: Phys. Rev. B **7**, 5313 (1973)
35. Barfield, W.D., Koontz, G.D., Huebener, W.F.: J. Quant. Spectr. Radiat. Transfer **12**, 1409 (1972)
36. Gelius, U.: Private communication
37. Kieser, J.: Physica Fennica **9**, Supplement S 1, 173 (1974)
38. Kortela, E.K., Manne, R. in: X-Ray Spectra and Electronic Structure of Matter, ed. A.Faessler and G.Wiech, München 1973, Vol. II, pp. 41–50
39. Kortela, E.K., Manne, R.: J. Phys. C **7**, 1749 (1974)
40. Pauling, L. in: The Nature of the Chemical Bond, p. 235. Ithaca, New York: Cornell University Press 1960
41. Borovskii, I.B., Matiskin, I., Nefedov, V.I.: Journal de Physique, Colloq. 32 (1971), C4–207
42. Müller, J., Feser, K., Wiech, G., Faessler, A.: Phys. Letters **44** A, 263 (1973)
43. Beyreuther, Ch., Wiech, G.: Physica Fennica **9**, Suppl. S1, 176 (1974)
44. Beyreuther, C., Hierl, R., Wiech, G.: Ber. Bunsenges. Phys. Chem. **79**, 1081 (1975)
45. McFarlane, A.A.: Carbon **11**, 73 (1973)

J. Kieser
Physikalisches Institut
der Universität Karlsruhe
Postfach 6380
D-7500 Karlsruhe 1
Federal Republic of Germany